Journal Pre-proof


# Physicochemical properties of films produced using nanoemulsions stabilized by carboxymethyl chitosan-peptide conjugates and application in blueberry preservation

Xinye Liu, Feng Xue, Chen Li, Benu Adhikari

PII: S0141-8130(21)02830-0

DOI: https://doi.org/10.1016/j.ijbiomac.2021.12.186

Reference: BIOMAC 20139

To appear in: *International Journal of Biological Macromolecules*

Received date: 20 October 2021

Revised date: 11 December 2021

Accepted date: 29 December 2021

Please cite this article as: X. Liu, F. Xue, C. Li, et al., Physicochemical properties of films produced using nanoemulsions stabilized by carboxymethyl chitosan-peptide conjugates and application in blueberry preservation, *International Journal of Biological Macromolecules* (2021), https://doi.org/10.1016/j.ijbiomac.2021.12.186

This is a PDF file of an article that has undergone enhancements after acceptance, such as the addition of a cover page and metadata, and formatting for readability, but it is not yet the definitive version of record. This version will undergo additional copyediting, typesetting and review before it is published in its final form, but we are providing this version to give early visibility of the article. Please note that, during the production process, errors may be discovered which could affect the content, and all legal disclaimers that apply to the journal pertain.

© 2022 Elsevier B.V. All rights reserved.

Title:

**Physicochemical properties of films produced using nanoemulsions stabilized by carboxymethyl chitosan-peptide conjugates and application in blueberry preservation**

Abbreviated running title:

**Chitosan-peptide conjugates containing essential oil**

Authors:

Xinye Liu[1, 2], Feng Xue[1*], Chen Li[3], Benu Adhikari[2]

Affiliations:

[1]School of Pharmacy, Nanjing University of Chinese Medicine, Nanjing 210023, PR China

[2]School of Science, RMIT University, Melbourne VIC 3083, Australia

[3]College of Food Science and Light Industry, Nanjing Tech University, Nanjing 211816, PR China

[*]Corresponding authors:

Email: xuefeng@njucm.edu.cn; benu.adhikari@rmit.edu.au

Journal Pre-proof

**Abstract:**

Carboxymethyl chitosan (CMCh)-peptide conjugates were produced by grafting CMCh with peptides from hemp seed, maize and casein. The nanoemulsions stabilized by these conjugates had smaller droplet size and better emulsifying properties. Nanoemulsions stabilized by conjugates were used to develop active films containing *Camellia* essential oil and the effect of conjugation on physicochemical properties of resulting films was evaluated. Water vapor and oxygen barrier properties, tensile strength, flexibility, and temperature of endothermic peak increased 6.6-19.8% and 6.9-27.2%, 40.1-96.6%, 61.4-83.3% and 7.8-18.5%, respectively when the CMCh-peptide conjugates were used to emulsify the essential oil. The conjugation helped to form compact structure. All of the films containing essential oil emulsions stabilized by conjugates showed the ability to extend the shelf-life of blueberry by maintaining the firmness, reducing the weight loss and slowing down the formation of soluble solids.

Keywords: Carboxyn ethyl chitosan; Peptides; Conjugates; Nanoemulsions; Films; Essential oil

Journal Pre-proof

## 1. Introduction

Chitosan is a natural linear biopolymer derived from partial deacetylation of chitin [1]. It has been widely used in food packaging to extend the shelf-life of fruits, vegetables, seafood and animal products due to its excellent film-forming properties and antimicrobial characteristics. For example, the chitosan-based films were shown to exhibit preservative effect on shrimp [2]. Beef fillets coated with chitosan-based films showed a substantially reduced the total viable count and better sensorial properties [3]. Chitosan-based films were also found to prolong the shelf life of bananas for ten days [4]. In non-food application, chitosan-based films are used as wound dressings, adsorbent materials to remove pollutants and antibacterial fabrics [5, 6]. However, a much broader application of chitosan is limited due its poor solubility in water. It needs to be dissolved in acetic acid solution, which can leave residual acetic acid in the final product and affect the sensory properties of the product.

A better solubility of chitosan in water can be achieved by introducing carboxymethyl groups to the amino and hydroxyl sites of the glucosamine [7]. In addition to improving water solubility, carboxymethyl chitosan (CMCh) also retains film-forming and antimicrobial properties of chitosan. Due to these reasons, CMCh is attracting increasingly research interest specially in food packaging application. For example, CMCh was used to prepare antifogging films which could extend the shelf-life of fruits by delaying the water loss at the same time reducing the growth of

microorganisms [8]. However, as CMCh is hydrophilic in nature, packaging and coating produced using CMCh come with substantially poor water barrier properties compared to synthetic plastic films, and thus, not favored in food packaging. This disadvantage can be overcome by incorporating lipids, i.e. producing emulsion-based films.

Emulsion-based films possess high water vapor barrier properties due to the presence of hydrophobic lipids. For the preparation of emulsion-based films, the emulsifying properties of film-forming materials play an important role as physicochemical properties of films depend on uniform distribution of lipid in the emulsion as well as in the film [9]. Previous study has shown that the emulsifying properties of CMCh could be improved by conjugating it with casein hydrolysate and using the conjugates to produce nanoemulsions [10]. However, no studies have undertaken to determine if these nanoemulsions can be used to prepare films and also to extend the shelf-life of foods.

In general, beeswax, vegetable oils and essential oils can be used to prepare emulsion-based films. Among these lipids, essential oils have shown to have excellent antioxidant and antimicrobial properties, which are important parameters for extending shelf-life of foods. For example, the essential oils from oregano, thyme, lemon, lemongrass, fruit *of Amomum tsaoko* Crevost et Lemaire, grapefruit and sage have been used to enhance the antioxidant and antimicrobial properties of emulsion-based films [9, 11]. Essential oils obtained from *Camellia japonica* are reported to have antioxidant activity due to the high level of squalene, flavonoids and

tocopherol [12]. However, there are few reports about its application in nanoemulsions-based films.

In this context, this study aimed to investigate the physicochemical properties of nanoemulsions-based films produced using CMCh-peptide conjugates loaded with *Camellia japonica* essential oil. In addition, the ability of these films in extending the shelf life of blueberry was also studied.

## 2. Materials and methods

### *2.1. Materials and chemicals*

Carboxymethyl chitosan (>80 % carboxylation, molecular weight = 150-800 KDa), essential oil from *Camellia japonica* (98 %) were purchased from Shanghai Yuanye biotechnology Co., Ltd (Shanghai, China). Solid-phase microextraction (SPME) coupled with gas chromatography mass spectrometry (GC-MS) was used to analyze main components in *Camellia japonica* essential oil. The details of methods, the chromatogram and identification of volatile compounds were shown in supplementary materials (Figure S1 and Table S1). The main constituents identified from database were myrtenol, α-terpineol, carvacrol and thymol. Glycerol was purchased from Macklin Biochemical Co., Ltd (Shanghai, China). Antioxidant peptide was prepared from hemp seed proteins by Alcalase at pH of 9.0 for 5 h according to our earlier study [13]. The antioxidant peptides obtained from maize (MP) and casein (CP) were

purchased from Guangzhou Honsea Industry Co., Ltd. (Guangdong, China) and Beijing Hongrunbao Science Co., Ltd. (Beijing, China), respectively. The molecular mass distribution of these peptide samples was measured according to our previous study [13] and the results are presented in supplementary material (Figure S2). The peptides were acid hydrolyzed at 110 °C for 24 h in 6 M HCl in vacuum-sealed tubes and the content of amino acids were determined by automatic amino acid analyzer (Biochrom, UK). The results were shown in supplementary material (Table S2). HT-29 (human colon carcinoma cell lines) were purchased from the Collection of Cell Cultures of the Fourth Military Medical University (Shaanxi, China). Dulbecco's modified Eagle medium (DMEM) was purchased from Thermo Fisher Scientific Inc. (Shanghai, China). The blueberries were purchased from local supermarket (Nanjing, China). The other reagents were purchased from Sinopharm Chemical Reagent Co., Ltd (Shanghai, China).

*2.2. Preparation of carboxymethyl chitosan-peptide conjugates*

The CMCh-peptide conjugates were prepared from each peptide sample according to our earlier study with minor modification [14]. Briefly, CMCh (5 g) and peptide (5 g) were dispersed in 100 mL phosphate buffer (10 mM, pH7.4) and stirred for 12 h at 4 °C. These well mixed dispersions were freeze-dried first at -50 ℃ and 1.3 Pa by FD-2B freezing dryer (Beijing Boyikang Experimental Instrument Co. Ltd., China). The freeze-dried samples are denoted as mixture of CMCh and peptides. CMCh/HP

denotes the mixture of CMCh and hemp seed peptides. CMCh/MP denotes the mixture of CMCh and maize peptides. CMCh/CP denotes the mixture of CMCh and casein peptides. The freeze-dried samples were incubated in a ventilated chamber (KBF720, Binder, Germany) at 60 °C and 79% relative humidity for 7 days, followed by freeze-drying using the same parameters mentioned above. The Maillard reaction products are defined as conjugates of CMCh and peptides. CMCh-HP denotes the conjugates of CMCh and hemp seed peptides. CMCh-MP denotes the the conjugates of CMCh and maize peptides. CMCh-CP denotes the conjugates of CMCh and casein peptides.

*2.3. Physicochemical properties of carboxymethyl chitosan-peptide conjugates*

The free amino groups in mixtures or conjugates were determined by o-Phthaldialdehyde (OPA) method as described in our previous study [15]. Briefly, 200 μL sample solution (2 mg/mL) was incubated with 4 mL of OPA reagent at 35 ℃ for 2 min and the absorbance at 340 nm was measured by using Spark 10M spectrophotometer (Tecan, Switzerland) to obtain the content of free amino groups. The lysine and arginine contents in the mixtures or conjugates were determined as described in Section 2.1. The decrease of free amino groups, lysine and arginine were calculated and used to evaluate degree of grafting. The absorbance of the conjugates (5 mg/mL) was measured at 420 nm as browning index. The L (lightness), a* (redness and greenness) and b* (yellowness and blueness) of conjugates were measured by

using a Hunter-Lab colorimeter (Reston, VA). To obtain the intrinsic tryptophan (Trp) fluorescence, conjugates solution (1 mg/mL) were excited at 285 nm and emission spectra were recorded from 300 to 600 nm by using Spark 10M spectrophotometer. The emulsifying activity index (EAI) and emulsion stability index (ESI) of conjugates were measured according to our previous study [16]. Briefly, 30 mL sample solution (2 mg/mL) and 10 mL oil were mixed and homogenized to obtain the emulsion. The EAI and ESI were measured immediately or 10 min after homogenization at 500 nm.

*2.4. Preparation of nanoemulsions stabilized by the carboxymethyl chitosan-peptide conjugates*

The conjugates (2 g) and glycerol (0.2 g) were dissolved in 100 mL distilled water by stirring for at least 12 h (4 °C). To prepare coarse emulsion, the essential oil (0.15 g) was added into the above solution and homogenized by using a homogenizer (FM200, FLUKO, China) operating at 10,000 rpm for 2 min. The coarse emulsion was further homogenized using ultrasound equipment (NingBo Scientz Biotechnology Co. Ltd., China) with a 0.636 cm diameter titanium probe at 400 W for 10 min. The fine emulsion was degassed by vacuuming (KEWEI, China) for at least 30 min.

*2.5. Characterization of nanoemulsions*

The droplet size and zeta potential of the nanoemulsions were measured by using a

nanosizer (Zetasizer Nano ZS90, Malvern Instruments Ltd., Malvern, UK). The refractive index and absorption parameter of water were 1.330 and 0.001, respectively. Cytotoxicity was determined by measuring the viability of cells in the presence of nanoemulsions following our previous study with minor modification [17]. HT-29 cells were seeded on 96-well plates and cultured for 72 h. Then, the cell culture medium was removed from each well. The 100 μL nanoemulsions diluted in 100 μL DMEM were added to each well, and the cells were incubated at 37 ℃ for 4 h. Finally, cell viability was determined by using the 3-[4, 5-Dimethylthiazol-2-yl]-2, 5-diphenyltetrazolium bromide (MTT) assay.

*2.6. Preparation of nanoemulsion based films*

The nanoemulsion based films were prepared by casting 60 g of nanoemulsions on leveled polytetrafluoroethylene plates (42×42 cm) and then dried at 30 ℃ and 43 % relative humidity using KBF720 chamber for 18 hours.

*2.7. Characterization of films*

The L, a* and b* of films were measured by using colorimeter and the lightness was calculated from those parameters according to equation 1.

$$\text{Lightness} = 100 - \sqrt{(100 - L^2) + a^{*2} + b^{*2}} \qquad (1)$$

The transparency of films was obtained by measuring the transmittance of light

through the film at 600 nm. The thickness of films was measured by using micrometer with the accuracy of 1 μm. The films were sealed on top of a permeation cup (open mouth of area: 1.33 ×$10^{-4}$ $m^2$) filled with anhydrous silica gel, and kept in a ventilated chamber maintained 75% at 25 °C. The cups were weighed at 2 h intervals and the water vapor permeability (WVP) was measured according to equation 2.

$$\text{WVP} = \frac{\Delta m \times x}{\Delta t \times A \times \Delta P} \quad (2)$$

Where, Δ m is the weight gain (g) of the cups during time Δt (s), x is the thickness of film (m), A ($m^2$) is the area of open mouth and ΔP (Pa) is the water vapor pressure differential across the film.

The oxygen barrier property was measured using an indirect method according to previous studies and the peroxide value (PV) was used to evaluate the oxygen barrier property of films [18, 19]. Deionized water (5 $\mu$L) was dropped on the films (20 ×20 mm) and the image was recorded to calculate the contact angle. The film was cut into rectangular strips (25 ×100 mm) and mechanical properties were measured by Rapid TA texture analyzer (Shanghai Tengba Instrument Co., Ltd, China) with an initial grip separation of 50 mm, a crosshead speed of 1 mm/s and using a load cell of 5 kg.

The films (2 cm× 2 cm) were scanned using IS5 spectroscope (Thermal Fisher Scientific, USA) with a horizontal ATR to obtain Fourier transform infrared spectra (FTIR) in the wavenumber range of 4000−500 $cm^{-1}$. X-ray diffraction (XRD) pattern of films (2 cm× 2 cm) were recorded using Ultima IV X-ray diffractometer (Rigaku, Japan) in the range of 10 to 80°(2θ). To study the thermal properties, the films (3-6 mg) were heated at a rate 10 °C $min^{-1}$ in an aluminum pan from 30 to 200 °C under $N_2$

atmosphere and the differential scanning calorimetry (DSC) curves were obtained by using thermal analyzer (TA Instruments, USA). The films (5 mg) were heated at a rate 10 °C $min^{-1}$ from 30 to 700 °C and thermogravimetric (TG) curves were obtained by using STA 2500 thermal analyzer (NETZSCH-Gerätebau GmbH, Germany). The surface and cross section morphology of films were obtained using SU8010 scanning electron microscope (HITACHI, Japan) at 5.0 kV acceleration voltage.

Indoor soil burial degradation was performed according to an earlier study with minor modification[20]. Films were cut into 1×1 cm size and buried in 500 g of moist soil collected from Nanjing University of Chines Medicine campus. The height of the soil bed was 20 cm and the films were placed at the depth of 10 cm. The soil bed and the samples were kept in a ventilated chamber maintained at 75 % RH and 25 °C for 30 days. After set degradation period, films were taken out from soil, rinsed with water to remove adhered soil, and dried at room temperature for 24 h. The microstructure of films was observed by microscope (DM2500, Leica, Germany).

*2.8. Application of films to preserve blueberries*

The blueberries were wrapped with one-layer of test films (10 cm × 10 cm) and stored at 4°C for 12 days. Weight loss and total soluble solids were measured according to Zhou et al.[21]. Briefly, weight loss during the storage was calculated by subtracting sample weight at specific time intervals (0, 4, 8 or 12 days) from their initial weight and presented as percentage. The portable refractometer (Suwei, China) was used to

determine the total soluble solids of the blueberry homogenates at specific time intervals (0, 4, 8 or 12 days). To evaluate the firmness, blueberry was punctured with a needle like probe by using Rapid TA texture analyzer. The firmness was obtained at speed of 1 mm/s and a load cell of 5 kg.

*2.9. Statistical analysis*

All of the tests mentioned above were performed in triplicate and the data obtained were analyzed by one-way analysis of variance using SPSS for Windows version 17.0 (IBM, USA). Values are expressed as mean ± standard deviation. Duncan's multiple range test was used to identify significant difference between two mean values at 95% confidence level ($p<0.05$).

## 3. Results and discussion

*3.1. Physicochemical properties of CMCh-peptide conjugates*

*3.1.1 Degree of grafting*

Maillard reaction between proteins and polysaccharides reduces the number of free amino groups. It has also been shown that free amino groups taking part in the grafting reaction mainly came from lysine and arginine of the proteins. Therefore, the

extent of decrease of free amino groups, and lysine and arginine in conjugates was used as an indicator of extent or progress of Maillard reaction. In general, the rate of Maillard reaction depends on the type of protein or polysaccharide used, the protein-to-polysaccharide ratio, and the reaction conditions (e.g. temperature, humidity and time). As shown in Fig. 1 A, the CMCh-CP conjugates possessed much higher DG values than CMCh-MP or CMCh-hemp peptide (HP) conjugates at the same reaction conditions, which indicated that the grafting reaction between CMCh and casein peptides progressed much faster than maize or hemp seed peptides. The higher Maillard reaction rate between CMCh and CP can be attributed to the lower molecular weight of casein peptides (350 Da, as shown in supplementary material Figure S2). Flexible structure and small size of casein peptides facilitates give rise to high mobility and faster reaction with CMCh. Previous studies have shown that a molecule with greater flexibility and mobility can much readily undergoes grafting reaction [14, 22].

*3.1.2 Browning index*

The grafting reaction between of proteins and polysaccharides can result into increased color intensity. Therefore, the browning index has been also widely used to quantify the degree of the grafting reaction [23]. As shown in Fig. 1 B, browning index in conjugates was much higher than in mixtures or the CMCh, which suggested that the peptides were grafted with CMCh. Furthermore, the browning index in

CMCh-CP conjugates was higher than in CMCh-MP or CMCh-HP conjugates. This result also indicated that the reaction between chitosan and casein peptides progressed to a greater degree, which is consistent with the observation made through DG values.

*3.1.3 Color parameters*

The color of conjugates was also measured by CIE Lab parameters. As shown in Fig. 1 C, the grafting reaction led to a decrease of lightness and an increase of redness and yellowness, which was also a clear indication of Maillard reaction taking place [15].

*3.1.4 Fluorescence intensity*

The intrinsic fluorescence can be used as an indicator of changes in protein tertiary structure and loss of amino group [24]. As shown in Fig. 1 D, the fluorescence intensity in conjugates was lower than in mixtures. The decrease in fluorescence intensity can be be attributed to the shielding effect of CMCh. It is assumed that Trp in conjugates is surrounded by larger number/amount of CMCh than in mixtures. On the other hand, the shielding effect in conjugates was stronger than in mixtures due to the fact that conjugates exhibited greater steric hindrance than mixtures [10]. Moreover, the CMCh-CP conjugates showed lower fluorescence intensity than CMCh-MP or CMCh-HP conjugates, which can be attributed to the higher degree of grafting CMCh-CP conjugates. This result indicated that the shielding effect increased

when a greater number of peptides was attached to CMCh.

*3.1.5 Molecular interactions*

The infrared spectra can be used to gain insight on the interactions between carboxymethyl chitosan and peptide molecules. As shown in Fig. 1 E, the band appearing at 3420 $cm^{-1}$ in mixtures or conjugate shifted to lower wavenumber, which indicated that the incorporation of peptides or grafting with peptides could affect the hydrogen bonds in carboxymethyl chitosan [25]. In the case of conjugates a new peak was observed at 1569 $cm^{-1}$ which can be attributed to the C=N stretching vibration originated from Maillard reaction between CH groups of CMCh and amino groups of peptides [6]. This result further confirmed that CMCh and peptides were successfully conjugated.

*3.1.6 Emulsifying properties*

As shown in Fig. 1 F, the EAI and ESI values of CMCh were improved remarkably after grafting with peptides. Th peptide residues attached on carbohydrate chain could rapidly adsorb to the oil-water interface which leads to greater stability of emulsions (higher EAI). Similar results have been observed in soy protein-gum acacia, peanut protein-glucomannan and buckwheat protein-dextran conjugates [14, 15, 26]. Gum acacia can be used as another example to explain this phenomenon that the presence

of peptides residue is the reason why gum acacia exhibits excellent emulsifying properties [27]. The improvement in ESI could be attributed to the tendency of conjugates to be closely packed and form thicker layer at the water-oil interface [28]. Moreover, CMCh-CP conjugates showed better emulsifying properties than CMCh-MP and CMCh-HP conjugates. This could be due to the fact that higher number of casein peptides were grafted to the CMCh chain (higher degree of grafting) and highly surface-active nature of CP, both of which make the CMCh-CP conjugates absorb to a greater degree at water-oil interface more rapidly and form a thicker interfacial layer.

*3.2. Properties and cytotoxicity of film-forming nanoemulsions*

Nanoemulsions can be prepared by using ultrasound, high pressure and rotor-stator type homogenization, and high pressure microfluidisation [29]. Among these methods, ultrasound homogenization is increasingly favored due to its simple and easy operation, high energy efficiency, affordability, and ability to produce stable emulsions. As shown in Fig. 2 A, emulsions stabilized by conjugates size (diameter) in the range of 200-500 nm, which is in accordance with the definition of nanoemulsions [30]. However, the size of emulsions stabilized by CMCh or its mixture with peptides were much higher (in the range of 901-937 nm), which might be due to insufficient amount of emulsifier absorbed at water-oil interface. Previous study has shown that the insufficient concentration of an emulsifier could result in emulsions with larger diameter [10]. As

compared with mixtures, conjugates exhibited higher degree of adsorption at the oil-water inter face, which could be attributed to the conjugates' ability to occupy higher proportion of interfacial area than mixtures due to their compact size [26]. Moreover, the nanoemulsions stabilized by conjugates also showed the decrease in surface charge (zeta potential) (Fig. 2 A), as compared with mixtures or carboxymethyl chitosan due to conjugation between CMCh and peptides. Previous studies have also shown that the complexation or conjugation between protein and polysaccharides can lead to a decrease or neutralization of surface charge [26, 28, 31]. In addition, the nanoemulsions stabilized by CMCh-CP conjugates showed smaller particle size and lower surface charges than CMCh-MP and CMCh-HP conjugates. This can be attributed to the higher degree of grafting (higher DG value) in CC-CP conjugates which enable them to absorb at the oil-water interface to a greater degree due to the reduction of electrostatic repulsion and also an increase in interface activity [26] .

The cytotoxicity of nanoemulsions to monolayer of HT 29 cells is shown in Fig. 2 B. It was found that there was no significant difference in the viability of cells among the different nanoemulsions. These results indicated that nanoemulsions had low toxicity and good biocompatibility and can be used to prepare edible films.

### *3.3. Physical properties of films*

#### *3.3.1. Lightness, transparency, thickness, water vapor permeability, surface*

*hydrophobicity and mechanical properties*

The films produced using conjugate stabilized nanoemulsions showed lower lightness value than those stabilized by CMCh and mixtures, which could be attributed to the presence of brown-colored compounds produced by Maillard reaction (Fig. 3A). This is consistent with earlier report that the films made of protein-polysaccharide conjugates had lower lightness than films made of protein/polysaccharide mixtures [32]. The type or nature peptides used significantly affected the lightness of conjugates films and the CMCh-CP films showed the lowest lightness, which could be due to the highest DG values in these conjugates.

As shown in Fig. 3 B, films produced by using emulsions stabilized by conjugates showed a decrease in transparency comparing with films produced by mixture-stabilized emulsions. Previous study has also shown that transparency of nanoemulsions-based films could be affected by film thickness and distribution of oil in the films [9]. As shown in Table 1, the thickness of films produced by conjugate-stabilized emulsions was not significantly ($P > 0.05$) different compared to those produced using mixture-stabilized emulsions. Therefore, the decrease in transparency in these films can be attributed to the distribution of oil in the films. As observed in Fig. 2, the particle (droplet) size of nanoemulsions stabilized by conjugates was much lower than nanoemulsions stabilized by mixtures, indicating that the oil was more evenly distributed in these films and eventually affecting the light scattering and transparency [11]. The presence of brown-colored compounds in

films produced by conjugate-stabilized emulsions is also expected to scatter and absorb light differently and then affect the film's transparency. Previous study has shown that the incorporation of pigmented compounds decreased the film's transparency [33]. The transparency of films was also affected by the type (nature) of peptide used and that the lowest transparency was observed in CMCh-CP films. This is because CMCh-CP conjugates possessed higher browning index than other conjugates and the nanoemulsions stabilized by CMCh-CP conjugates showed lower particle size (and better oil distribution) than those stabilized by other conjugates. In addition, the appearance of films was consistent with the lightness and transparency (Fig. 3 C).

As shown in Table 1, films produced using emulsions stabilized by conjugates showed lower WVP comparing to the ones produced by mixture-stabilized emulsions. In general, the water vapor barrier properties of emulsion-based films depend on surface hydrophobicity and intermolecular interactions. Our data showed that the contact angle of the films prepared using conjugate-stabilized emulsion was not significantly ($P > 0.05$) different compared to those produced using emulsions stabilized by the mixtures (Table 1). Therefore, the decrease in WVP could be attributed to the conjugation between CMCh and peptides which produces more compact structure than mixtures. Previous studies have shown that conjugation between proteins and polysaccharides or incorporation of cross-linker improves the water vapor barrier properties of films by consolidation of the network structure [32, 34]. The films prepared from conjugate-stabilized emulsions also showed lower PV compared to the

ones prepared from mixture-stabilized emulsions (Table 1), indicating an improvement in oxygen barrier property. This improvement of oxygen barrier property can also be attributed the more compact structure induced by enhanced molecular interaction in conjugates. Previous study showed that greater molecular interaction between components in the films resulted into close-knit (compact) network in films which ultimately resulted into increased oxygen barrier [21]. The films produced by CMCh-CP conjugate stabilized emulsions showed the lowest WVP and the best oxygen barrier property than other films, which can be related to higher degree of covalent crosslinking between CMCh and CP.

Incorporation of peptides increased the tensile strength in films compared to that of the control (CMCh films) (Table 1). This increase can be due to the formation of noncovalent bonds (electrostatic and/or hydrogen bonds) between the carboxymethyl chitosan and peptides. Noncovalent bonds helped create a more rigid network, thereby increased the tensile strength of the films. This is consistent with previous study that more compact network in films increases the tensile strength [35]. As compared with the films prepared from emulsions stabilized by mixtures, the ones prepared from emulsion stabilized by conjugates possessed higher tensile strength, which indicated that the Maillard reaction induced glycation further enhanced the intermolecular interactions. It is likely for flexibility (elongation) to decrease when the tensile in packaging films increases [11]. This theory was confirmed by our data that mixtures films possessed lower flexibility than that of control (CMCh films). However, the films produced using CMCh-peptide conjugates showed higher tensile strength as

well as the flexibility (EB) than those prepared from mixtures. The increase in flexibility can be attributed to the much smaller droplet size and more uniform distribution of essential oil film-forming nanoemulsions. This observation is consistent with previous study that droplet size of film-forming nanoemulsions could affect the flexibility of films by changing the distribution of oil in film matrix [9].

*3.3.2. Chemical interactions among the components of the films*

The FTIR spectra of all the tested films along with marked peaks of interest are presented in Fig. 4A. The peaks at around 1550 $cm^{-1}$ and 1410 $cm^{-1}$ are attributed to antisymmetric and symmetric vibrations for COO- group, respectively [21]. The peak at around 1042 $cm^{-1}$ is attributed to C-O-C groups. When compared with CMCh films, incorporation of peptides decreased the intensity of band at 1550 $cm^{-1}$, which can be attributed to the interaction between carboxyl group of chitosan and amino group of peptides. The intensity of band at 1550 $cm^{-1}$ in films produced from CMCh-conjugate stabilized emulsion was weaker than mixtures films produced using mixture-stabilized emulsions, which can be attributed to the crosslinking induced by Maillard reaction [36]. The intensity of band at 3265 $cm^{-1}$ was lower in films produced by emulsions stabilized by mixture and conjugate when compared with that in CMCh films, indicating that the intramolecular hydrogen bonds in CMCh might be disrupted. This could be attributed to the formation of new interactions between CMCh and peptides.

*3.3.3. X-ray diffraction patterns*

As shown in Fig. 4 B, the CMCh films exhibited diffraction peak (2θ) at 20°, which could be attributed to the characteristic structure of CMCh [37]. The diffraction peak became sharper and shifted to the left after incorporation of peptides. This shift indicated that incorporation of peptides altered the native crystalline domains of CMCh. This alteration could be attributed to intermolecular interactions between CMCh and peptides. Moreover, the diffraction peak in conjugates films was sharper than that in mixtures films, which could be attributed to the crosslinking induced by Maillard reaction. This also explains why WVP was significantly lower in these films. As crystalline domains are less permeable to water vapor transfer

*3.3.4. Thermal properties*

CMCh films (Fig. 4C) exhibited two main stages of mass loss. The initial loss below 150 ℃ was due to the evaporation of moisture and volatilization of essential oil [18]. The second mass loss at 150-300 ℃ was associated with the evaporation of glycerol and the thermal degradation of CMCh [21]. Three stages of degradation were observed in the films produced from emulsions stabilized by mixtures or conjugates. The initial mass loss below 100 ℃ can be attributed to the loss of moisture due to evaporation. In this stage, the temperature at which peak (highest level) vaporization

occurred was higher in the films produced using conjugate-stabilized emulsions than those produced using emulsions stabilized by mixtures. This can be attributed to the covalent conjugation induced crosslinking between CMCh and peptides, which has led to the formation of compact structure. This result is consistent with the observation made on DSC data (Fig. 4 D) that the endothermic peak shifted to higher temperature in conjugates films as compared with films produced using mixtures. The second stage of mass loss occurring between 150 and 250 °C can be attributed to the volatilization of essential oil and evaporation of glycerol. The films produced from conjugate-stabilized emulsions also showed higher temperature for volatilization of essential oil evaporation of glycerol evaporation as compared with the films produced using mixture-stabilized emulsions. The third stage of mass loss observed between 250°C and 350 °C can be attributed to the decomposition of CMCh and peptides [25, 38]. In this stage, the films produced from emulsions stabilized by CMCH-CP conjugates exhibited higher temperature of maximum degradation ($T_{max}$) than others, which indicated the better thermal resistance in the former. This higher thermal stability can be attributed to the covalent crosslinking between CMCh and casein peptides.

*3.3.5. Microstructure of films*

As shown in Fig. 5, incorporation of peptides or covalently crosslinked conjugates had no effect on the surface of films, which also helps explaining why all of these

films had similar surface hydrophobicity (Table 1). Previous studies have shown that the surface hydrophobicity of films depend on the microstructure of films and the rougher surface can lead to higher surface hydrophobicity [11, 33]. The microstructure of the film (seen from cross section) was greatly affected by incorporation of peptides as well as the covalently crosslinked conjugates. A multilayered structure and phase separation were observed in in films produced from CMCh-stabilized emulsions. This observation corroborates the higher loss of moisture and essential oil in these films than others (Fig. 4 C). The phase separation was not observed in films produced using emulsions stabilized by mixtures; however, non-uniform distribution of oil droplet was observed. When compared with these films (produced from emulsions stabilized by mixtures) the structure (observed through cross section) of films produced using emulsions stabilized with conjugates was more compact and uniform, which can be attributed to the enhanced intermolecular interaction and better emulsifying properties of conjugates. This greatly compact and uniform structure also explained why films produced from conjugate stabilized emulsions exhibited better barrier and mechanical properties (Table 1).

*3.6. Biodegradability of the films*

Microstructure of all the films before and after 30 days of soil burial are shown in Fig. 6. Overall, all the films lost their initial appearance and structural integrity and

showed rougher and eroded surface morphology with dip pits, eroded region and cracks indicating a considerable level of biodegradation caused by microorganisms present in the soil. Therefore, all the films can be considered as biodegradable in nature. This observation is also supported by the fact that each of the components of the films are from biological source and are known to be biodegradable.

*3.7. Application of films on the preservation of blueberry*

The weight loss of fruits, induced by transpiration and respiration, leads to shrinkage and deterioration of fruits [39]. As shown in Fig. 7 A, all blueberry samples showed the continuous weight loss during storage. The unpackaged sample (control) showed higher weight loss than the samples wrapped in films, due to direct exposure to the environment. The weight loss slowed down in packaged samples, due to the moisture barrier property of the films. As compared with the films produced using mixture-stabilized emulsions, the ones produced using conjugate-stabilized emulsions showed significantly reduced weight loss and the CMCh-CP based films showed the lowest weight loss. This substantial reduction in weight loss can be attributed to the better barrier properties of conjugates films than other films. It is expected for the films with lower gas and vapor penetrability to reduce the weight loss in fruits and vegetables during the storage [21]. The weight loss was also intuitively reflected in supplementary material (Figure S3) that there was obvious shrinkage on the surface of blueberries coated with CMCh or CMCh/peptides films.

The firmness of all the blueberry samples showed a decreasing trend during storage (Fig. 7 B) which can be attributed to deterioration of cell wall components [40]. Blueberry samples packed in films slowed down the loss of firmness. The preservation of firmness could be attributed to slowing of the metabolic activity and maturation process. The coating with films is shown to retard maturation process of fruits by restricting the gas and moisture exchange though skin of fruits [41]. Among packaged blueberries, the firmness of samples packaged with conjugate films decreased more slowly than those packaged with mixed matrix. This could be attributed to the better barrier properties of conjugate matrix (Table 1).

Total soluble solids are widely used as an indicator of fruits ripening. The total soluble solids of all samples (Fig. 7 C) showed an increasing trend during the storage due to the hydrolysis of cell wall induced by increased respiration and microbial action. Packing of the blueberry samples in films slowed down the increase in total soluble solids during storage, which can be attributed to the barrier and antimicrobial properties of films. Previous study has shown that films with good antimicrobial and oxygen barrier properties were able to slow down the respiration and hydrolysis of tissues in fruits [21]. The antimicrobial activity of films can be attributed to the presence of *camellia* essential oil. It is shown that the phenolic compounds in *camellia* essential oil inhibit the growth of microorganism by binding with protein binding and inhibiting enzyme of microorganism [42]. The total soluble solids of blueberries packaged in conjugates films showed the slowest increasing trend than those packaged in CMCh and peptide mixture films, which could be attributed to the

better barrier (Table 1) and antimicrobial properties of the former. Previous study has shown that the Maillard reaction products from maize peptides and saccharide exhibited noteworthy antimicrobial activity [43].

## 4. Conclusion

The carboxymethyl chitosan (CMCh) was conjugated with three type of peptides through Maillard reaction. The conjugation reaction between CMCh and casein peptides was much faster than hemp seed or maize peptides. The nanoemulsions stabilized by CMCh-casein peptide conjugates had the smallest droplet and excellent emulsifying properties. The better emulsifying properties of CMCh-casein peptide conjugates and resulting small droplet size produced nanoemulsions-based films with more compact and homogeneous structure due to the more uniform distribution of oil droplets and enhanced molecular interaction. The films produced using emulsions stabilized by CMCh-peptide conjugates exhibited better barrier properties, mechanical properties and thermal resistance. The films produced using conjugates of CMCh-casein peptides by incorporating essential oil were also effective in extending the shelf-life of blueberry.

**Acknowledgments:** This work was supported by The Open Project of Chinese Materia Medica First-Class Discipline of Nanjing University of Chinese Medicine (2020YLXK021), The Natural Science Foundation of the Jiangsu Higher Education

Institutions of China (20KJB550014) and The Natural Science Foundation of Jiangsu Province (BK20171066).

**Consent for publication:** All authors consent to publish.

**Competing interests:** The authors declare no conflict of interest.

Journal Pre-proof

## References

[1] H. Haghighi, F. Licciardello, P. Fava, H.W. Siesler, A. Pulvirenti, Recent advances on chitosan-based films for sustainable food packaging applications, Food Packaging and Shelf Life 26 (2020) 100551.

[2] W. Liu, J. Xie, L. Li, B. Xue, X. Li, J. Gan, Z. Shao, T. Sun, Properties of phenolic acid-chitosan composite films and preservative effect on Penaeus vannamei, Journal of Molecular Structure 1239 (2021) 130531.

[3] K. Alirezalu, S. Pirouzi, M. Yaghoubi, M. Karimi-Dehkordi, S. Jafarzadeh, A. Mousavi Khaneghah, Packaging of beef fillet with active chitosan film incorporated with ε-polylysine: An assessment of quality indices and shelf life, Meat Science 176 (2021) 108475.

[4] Y. Ni, H. Nie, J. Wang, J. Lin, Q. Wang, J. Sun, W. Zhang, J. Wang, Enhanced functional properties of chitosan films incorporated with curcumin-loaded hollow graphitic carbon nitride nanoparticles for bananas preservation, Food Chemistry 366 (2022) 130539.

[5] F.P. de Freitas, A.M.M.L. Carvalho, A.d.C.O. Carneiro, M.A. de Magalhães, M.F. Xisto, W.D. Canal, Adsorption of neutral red dye by chitosan and activated carbon composite films, Heliyon 7(7) (2021) e07629.

[6] C.P. Li, Jiliu; Zhu, Shengyu; Song, Yukang; Xiong, Xiaohui; Xue, Feng., Development of Chitosan/Peptide Films: Physical, Antibacterial and Antioxidant Properties, Coatings 10(12) (2020) 1193.

[7] A.L. Bukzem, R. Signini, D.M. dos Santos, L.M. Lião, D.P.R. Ascheri, Optimization of carboxymethyl chitosan synthesis using response surface methodology and desirability function, International Journal of Biological Macromolecules 85 (2016) 615-624.

[8] L. Wen, Y. Liang, Z. Lin, D. Xie, Z. Zheng, C. Xu, B. Lin, Design of multifunctional food packaging films based on carboxymethyl chitosan/polyvinyl alcohol crosslinked network by using citric acid as crosslinker, Polymer (2021) 124048.

[9] A. Acevedo-Fani, L. Salvia-Trujillo, M.A. Rojas-Graü, O. Martín-Belloso, Edible films from essential-oil-loaded nanoemulsions: Physicochemical characterization and antimicrobial properties, Food Hydrocolloids 47 (2015) 168-177.

[10] L. Wang, S. Zhang, W. Jiang, H. Zhao, J. Fu, Ability of casein hydrolysate-carboxymethyl chitosan conjugates to stabilize a nanoemulsion: Improved freeze-thaw and pH stability, Food Hydrocolloids 101 (2020) 105452.

[11] F. Xue, Y. Gu, Y. Wang, C. Li, B. Adhikari, Encapsulation of essential oil in emulsion based edible films prepared by soy protein isolate-gum acacia conjugates, Food Hydrocolloids 96 (2019) 178-189.

[12] G. Ramachandran, G.N. Rajivgandhi, S. Murugan, N.S. Alharbi, S. Kadaikunnan, J.M. Khaled, T.N. Almanaa, N. Manoharan, W.-J. Li, Anti-carbapenamase activity of Camellia japonica essential oil against isolated carbapenem resistant klebsiella pneumoniae (MN396685), Saudi Journal of Biological Sciences 27(9) (2020) 2269-2279.

[13] S. Wang, J. Wang, F. Xue, C. Li, Effects of heating or ultrasound treatment on the enzymolysis and the structure characterization of hempseed protein isolates, Journal of Food Science and Technology 56(7) (2019) 3337-3346.

[14] F. Xue, C. Li, X. Zhu, L. Wang, S. Pan, Comparative studies on the physicochemical properties of soy protein isolate-maltodextrin and soy protein isolate-gum acacia conjugate prepared through Maillard reaction, Food Research International 51(2) (2013) 490-495.

[15] C. Li, X. Huang, Q. Peng, Y. Shan, F. Xue, Physicochemical properties of peanut protein isolate–glucomannan conjugates prepared by ultrasonic treatment, Ultrasonics Sonochemistry 21(5) (2014) 1722-1727.

[16] F. Xue, C. Zhu, F. Liu, S. Wang, H. Liu, C. Li, Effects of high-intensity ultrasound treatment on functional properties of plum (Pruni domesticae semen) seed protein isolate, Journal of the Science of Food and Agriculture 98(15) (2018) 5690-5699.

[17] C. Li, J. Wang, J. Shi, X. Huang, Q. Peng, F. Xue, Encapsulation of tomato oleoresin using soy protein isolate-gum aracia conjugates as emulsifier and coating materials, Food Hydrocolloids 45 (2015) 301-308.

[18] K. Zhang, W. Wang, K. Zhao, Y. Ma, S. Cheng, J. Zhou, Z. Wu, Producing a novel edible film from mushrooms (L. edodes and F. velutipes) byproducts with a two-stage treatment namely grinding and bleaching, Journal of Food Engineering 275 (2020) 109862.

[19] A. Kurt, T. Kahyaoglu, Characterization of a new biodegradable edible film made from salep glucomannan, Carbohydrate Polymers 104 (2014) 50-58.

[20] A.R. Deshmukh, H. Aloui, C. Khomlaem, A. Negi, J.-H. Yun, H. S. Kim, B.S. Kim, Biodegradable films based on chitosan and defatted Chlorella biomass: Functional and physical characterization, Food Chemistry 337 (2021) 127777.

[21] W. Zhou, Y. He, F. Liu, L. Liao, X. Huang, R. Li, Y. Zou, L. Zhou, L. Zou, Y. Liu, R. Ruan, J. Li, Carboxymethyl chitosan-pullulan edible films enriched with galangal essential oil: Characterization and application in mango preservation, Carbohydrate Polymers 256 (2021) 117579.

[22] J.-J. Guan, A.-Y. Qiu, X.-Y. Liu, Y.-F. Hua, Y.-H. Ma, Microwave improvement of soy protein isolate–saccharide graft reactions, Food Chemistry 97(4) (2006) 577-585.

[23] B. Bi, H. Yang, Y. Fang, K. Nishinari, G.O. Phillips, Characterization and emulsifying properties of β-lactoglobulin-gum Acacia Seyal conjugates prepared via the Maillard reaction, Food Chemistry 214 (2017) 614-621.

[24] C. Li, H. Xue, Z. Chen, Q. Ding, X. Wang, Comparative studies on the physicochemical properties of peanut protein isolate–polysaccharide conjugates prepared by ultrasonic treatment or classical heating, Food Research International 57 (2014) 1-7.

[25] K. Wang, K. Wu, M. Xiao, Y. Kuang, H. Corke, X. Ni, F. Jiang, Structural characterization and properties of konjac glucomannan and zein blend films, International Journal of Biological Macromolecules 105 (2017) 1096-1104.

[26] F. Xue, Z. Wu, J. Zhong, J. Zheng, C. Li, Effect of combination of high-intensity ultrasound treatment and dextran glycosylation on structural and interfacial properties of buckwheat protein isolates, Biosci Biotechnol Biochem 81(10) (2017) 1891-1898.

[27] Y. Minemoto, K. Hakamata, S. Adachi, R. Matsuno, Oxidation of linoleic acid encapsulated with gum arabic or maltodextrin by spray-drying, Journal of Microencapsulation 19(2) (2002) 181-189.

[28] W. Li, H. Zhao, Z. He, M. Zeng, F. Qin, J. Chen, Modification of soy protein hydrolysates by Maillard reaction: Effects of carbohydrate chain length on structural and interfacial properties, Colloids and Surfaces B: Biointerfaces 138 (2016) 70-77.

[29] F. Xue, X. Li, L. Qin, X. Liu, C. Li, B. Adhikari, Anti-aging properties of phytoconstituents and phyto-nanoemulsions and their application in managing aging-related diseases, Advanced Drug Delivery Reviews (2021) 113886.

[30] G. Ren, Z. Sun, Z. Wang, X. Zheng, Z. Xu, D. Sun, Nanoemulsion formation by the phase inversion temperature method using polyoxypropylene surfactants, Journal of Colloid and Interface

Science 540 (2019) 177-184.
[31] B. Wang, E. Blanch, C.J. Barrow, B. Adhikari, Preparation and study of digestion behavior of lactoferrin-sodium alginate complex coacervates, Journal of Functional Foods 37 (2017) 97-106.
[32] C. Li, L. Wang, F. Xue, Effects of Conjugation between Proteins and Polysaccharides on the Physical Properties of Emulsion-Based Edible Films, Journal of the American Oil Chemists' Society 96(11) (2019) 1249-1263.
[33] F. Xue, M. Zhao, X. Liu, R. Chu, Z. Qiao, C. Li, B. Adhikari, Physicochemical properties of chitosan/zein/essential oil emulsion-based active films functionalized by polyphenols, Future Foods 3 (2021) 100033.
[34] H.-C. Lin, B.-J. Wang, Y.-M. Weng, Development and characterization of sodium caseinate edible films cross-linked with genipin, LWT 118 (2020) 108813.
[35] F. Garavand, M. Rouhi, S.H. Razavi, I. Cacciotti, R. Mohammadi, Improving the integrity of natural biopolymer films used in food packaging by crosslinking approach: A review, International Journal of Biological Macromolecules 104 (2017) 687-707.
[36] S. Affes, R. Nasri, S. Li, T. Thami, A. Van Der Lee, M. Nasri, H. Maalej, Effect of glucose-induced Maillard reaction on physical, structural and antioxidant properties of chitosan derivatives-based films, Carbohydrate Polymers 255 (2021) 117341.
[37] M. Zhao, H. Zhou, L. Chen, L. Hao, H. Chen, X. Zhou, Carboxymethyl chitosan grafted trisiloxane surfactant nanoparticles with pH sensitivity for sustained release of pesticide, Carbohydrate Polymers 243 (2020) 116433.
[38] S. Zhang, C. Xia, Y. Dong, Y. Yan, J. Li, S. Shi, L. Cai, Soy protein isolate-based films reinforced by surface modified cellulose nanocrystal, Industrial Crops and Products 80 (2016) 207-213.
[39] B. Niu, P. Shao, H. Chen, P. Sun, Structural and physiochemical characterization of novel hydrophobic packaging films based on pullulan derivatives for fruits preservation, Carbohydrate Polymers 208 (2019) 276-284.
[40] A. Boonsiriwit, Y. Xiao, J. Jeong, M. Kim, S. Singh, Y.S. Lee, Alkaline halloysite nanotubes/low density polyethylene nanocomposite films with increased ethylene absorption capacity: Applications in cherry tomato packaging, Food Packaging and Shelf Life 25 (2020) 100533.
[41] B. Hassan, S.A.S. Chatha, A.I. Hussain, K.M. Zia, N. Akhtar, Recent advances on polysaccharides, lipids and protein based edible films and coatings: A review, International Journal of Biological Macromolecules 109 (2018) 1095-1107.
[42] X. Zhou, X. Zong, M. Zhang, Q. Ge, J. Qi, J. Liang, X. Xu, G. Xiong, Effect of konjac glucomannan/carrageenan-based edible emulsion coatings with camellia oil on quality and shelf-life of chicken meat, International Journal of Biological Macromolecules 183 (2021) 331-339.
[43] T. Feng, Y. Zhou, X. Wang, X. Wang, S. Xia, α-Dicarbonyl compounds related to antimicrobial and antioxidant activity of maillard reaction products derived from xylose, cysteine and corn peptide hydrolysate, Food Bioscience 41 (2021) 100951.

**Figure captions:**

Fig. 1 Degree of grafting (A), browning index (B), color parameters (C), fluorescence intensity (D), FTIR spectra (E) and emulsifying properties (F) of carboxymethyl chitosan (CMCh), mixtures of CMCh and peptides and conjugates of CMCh-peptide. CMCh/HP: mixtures of CMCh and hemp seed peptides (HP); CMCh-HP: conjugates; CMCh /MP: mixtures of CMCh and maize peptides (MP); CMCh -MP: conjugates; CMCh /CP: mixtures of CMCh and casein peptides (CP); CMCh-CP: conjugates. Results having different letters in same pattern are significantly different ($p < 0.05$).

Fig. 2 Size and zeta potential (surface charge) of nanoemulsions stabilized by carboxymethyl chitosan (CMCh), mixtures of CMCh and peptides and CMCh-peptide conjugates. CMCh/HP: mixtures of CMCh and hemp seed peptides (HP); CMCh-HP conjugates; CMCh/MP: mixtures of CMCh and maize peptides (MP); CMCh-MP conjugates; CMCh/CP: mixtures of CMCh and casein peptides (CP); CMCh-CP conjugates. Results having different letters in size and zeta potential data are significantly different ($p < 0.05$).

Fig. 3 Lightness (A), transparence (B) and image (C) of nanoemulsions-based films prepared by carboxymethyl chitosan (CMCh), mixtures of CMCh and peptides and CMCh-peptide conjugates. CMCh/HP: mixtures of CMCh and hemp seed peptides

(HP); CMCh-HP conjugates; CMCh/MP: mixtures of CMCh and maize peptides (MP); CMCh-MP conjugates; CMCh/CP: mixtures of CMCh and casein peptides (CP); CMCh-CP conjugates. Results having different letters in same pattern are significantly different ($p < 0.05$).

Fig. 4 FTIR spectra (A), XRD patterns (B), DTG thermograms (C) and DSC curves (D) of nanoemulsions-based films prepared by carboxymethyl chitosan (CMCh), mixtures of CMCh and peptides and CMCh-peptide conjugates. CMCh/HP: mixtures of CMCh and hemp seed peptides (HP); CMCh-HP conjugates; CMCh/MP: mixtures of CMCh and maize peptides (MP); CMCh-MP conjugates; CMCh/CP: mixtures of CMCh and casein peptides (CP); CMCh-CP conjugates.

Fig. 5 SEM images of the surface and cross section of nanoemulsions-based films prepared by carboxymethyl chitosan (CMCh), mixtures of CMCh and peptides and CMCh-peptide conjugates. CMCh/HP: mixtures of CMCh and hemp seed peptides (HP); CMCh-HP conjugates; CMCh/MP: mixtures of CMCh and maize peptides (MP); CMCh-MP conjugates; CMCh/CP: mixtures of CMCh and casein peptides (CP); CMCh-CP conjugates.

Fig. 6 Microstructure of nanoemulsions-based films prepared by carboxymethyl chitosan (CMCh), mixtures of CMCh and peptides and CMCh-peptide conjugates at day 0 and after 30 days buried in soil. CMCh/HP: mixtures of CMCh and hemp seed

peptides (HP); CMCh-HP conjugates; CMCh/MP: mixtures of CMCh and maize peptides (MP); CMCh-MP conjugates; CMCh/CP: mixtures of CMCh and casein peptides (CP); CMCh-CP conjugates.

Fig. 7 Weight loss (A), firmness (B) and total soluble solids (C) of blueberry coated with nanoemulsions-based films prepared by carboxymethyl chitosan (CMCh), mixtures of CMCh and peptides and CMCh-peptide conjugates. CMCh/HP: mixtures of CMCh and hemp seed peptides (HP); CMCh-HP conjugates; CMCh/MP: mixtures of CMCh and maize peptides (MP); CMCh-MP conjugates; CMCh/CP: mixtures of CMCh and casein peptides (CP); CMCh-CP conjugates.

Journal Pre-proof

Table 1 Thickness, water vapor permeability (WVP), peroxide value (PV), contact angle, tensile strength (TS) and elongation at break (EB) of nanoemulsions- based films prepared by carboxymethyl chitosan (CMCh), mixtures of CMCh and peptides and CMCh-peptide conjugates.

| Sample | Thickness (μm) | WVP g/(m·s·Pa)×10$^{-9}$ | PV (meq/kg) | Contact angle ($^0$) | TS (MPa) | EB (%) |
|---|---|---|---|---|---|---|
| CMCh | 65.6±2.1$^{a}$ | 1.91±0.05$^{cd}$ | 90.51±2.16$^{c}$ | 71.55±3.04$^{a}$ | 1.83±0.13$^{a}$ | 90.4±3.6$^{d}$ |
| CMCh/HP | 68.7±3.0$^{a}$ | 1.97±0.05$^{d}$ | 94.21±2.67$^{c}$ | 73.47±3.67$^{a}$ | 4.39±0.31$^{c}$ | 60.0±4.1$^{a}$ |
| CMCh-HP | 68.2±1.9$^{a}$ | 1.84±0.02$^{b}$ | 87.69±2.07$^{b}$ | 74.56±4.06$^{a}$ | 6.15±0.39$^{d}$ | 110.0±5.7$^{e}$ |
| CMCh/MP | 70.1±5.1$^{a}$ | 1.94±0.04$^{d}$ | 93.57±4.98$^{c}$ | 74.68±1.96$^{a}$ | 3.28±0.17$^{b}$ | 70.2±2.9$^{b}$ |
| CMCh-MP | 68.9±1.8$^{a}$ | 1.85±0.03$^{bc}$ | 82.87±3.47$^{b}$ | 75.33±3.99$^{a}$ | 6.45±0.22$^{d}$ | 113.3±6.7$^{e}$ |
| CMCh/CP | 71.6±4.1$^{a}$ | 1.92±0.05$^{d}$ | 96.59±3.14$^{c}$ | 73.47±4.06$^{a}$ | 4.51±0.24$^{c}$ | 80.9±4.8$^{c}$ |
| CMCh-CP | 66.5±3.6$^{a}$ | 1.54±0.04$^{a}$ | 70.54±3.41$^{a}$ | 78.19±4.05$^{a}$ | 7.76±0.31$^{e}$ | 130.9±6.0$^{f}$ |

CMCh/HP: mixtures of CMCh and hemp seed peptides (HP); CMCh-HP conjugates; CMCh/MP: mixtures of CMCh and maize peptides (MP); CMCh-MP conjugates; CMCh/CP: mixtures of CMCh and casein peptides (CP); CMCh-CP conjugates.

Results having different letters within a column are significantly different ($p < 0.05$).

Journal Pre-proof

Author Statement

Conceptualization, methodology and investigation, Xinye Liu, Feng Xue, Chen Li and Benu Adhikari.

Writing original draft and review & editing, Xinye Liu and Feng Xue.

Project administration and funding acquisition, Feng Xue.

Graphical abstract

Journal Pre-proof

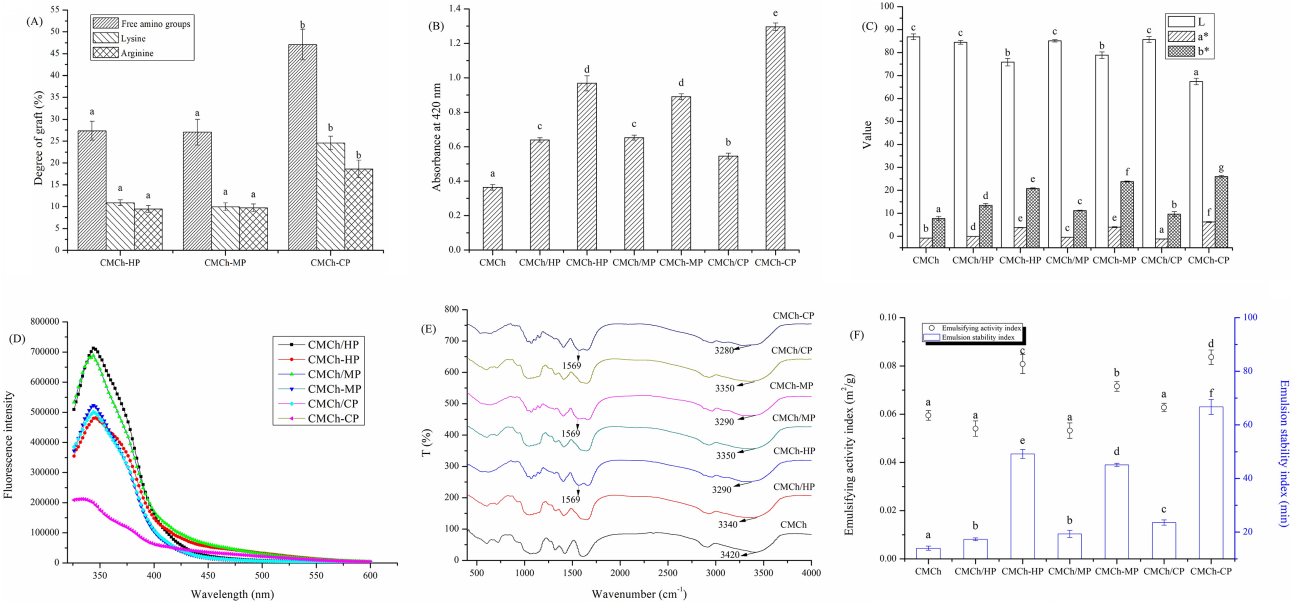
(A)
Free amino groups
Lysine
Arginine
Degree of graft (%)
CMCh-HP
CMCh-MP
CMCh-CP
(B)
Absorbance at 420 nm
CMCh
CMCh/HP
CMCh-HP
CMCh/MP
CMCh-MP
CMCh/CP
CMCh-CP
(C)
L
a*
b*
Value
(D)
CMCh/HP
CMCh-HP
CMCh/MP
CMCh-MP
CMCh/CP
CMCh-CP
Fluorescence intensity
Wavelength (nm)
(E)
T (%)
1569
3280
3350
3290
3340
3420
Wavenumber (cm-1)
(F)
Emulsifying activity index
Emulsion stability index
Emulsifying activity index (m2/g)
Emulsion stability index (min)

Figure 1

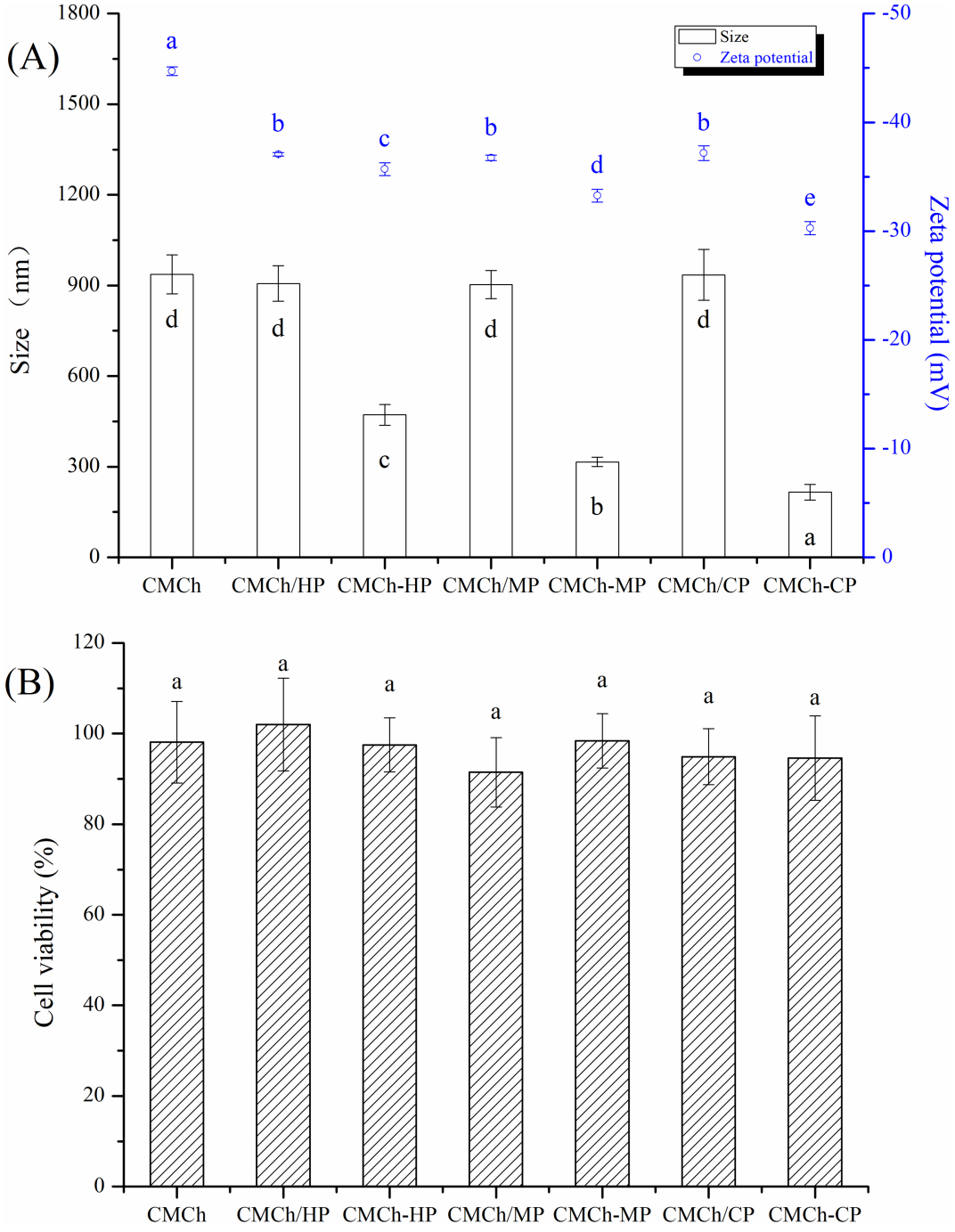
(A)
Size
Zeta potential
Size （nm）
Zeta potential (mV)
1800
1500
1200
900
600
300
0
-50
-40
-30
-20
-10
0
a
b
c
b
d
b
e
d
d
c
d
b
d
a
CMCh
CMCh/HP
CMCh-HP
CMCh/MP
CMCh-MP
CMCh/CP
CMCh-CP
(B)
Cell viability (%)
120
100
80
60
40
20
0
a
a
a
a
a
a
a
CMCh
CMCh/HP
CMCh-HP
CMCh/MP
CMCh-MP
CMCh/CP
CMCh-CP

Figure 2

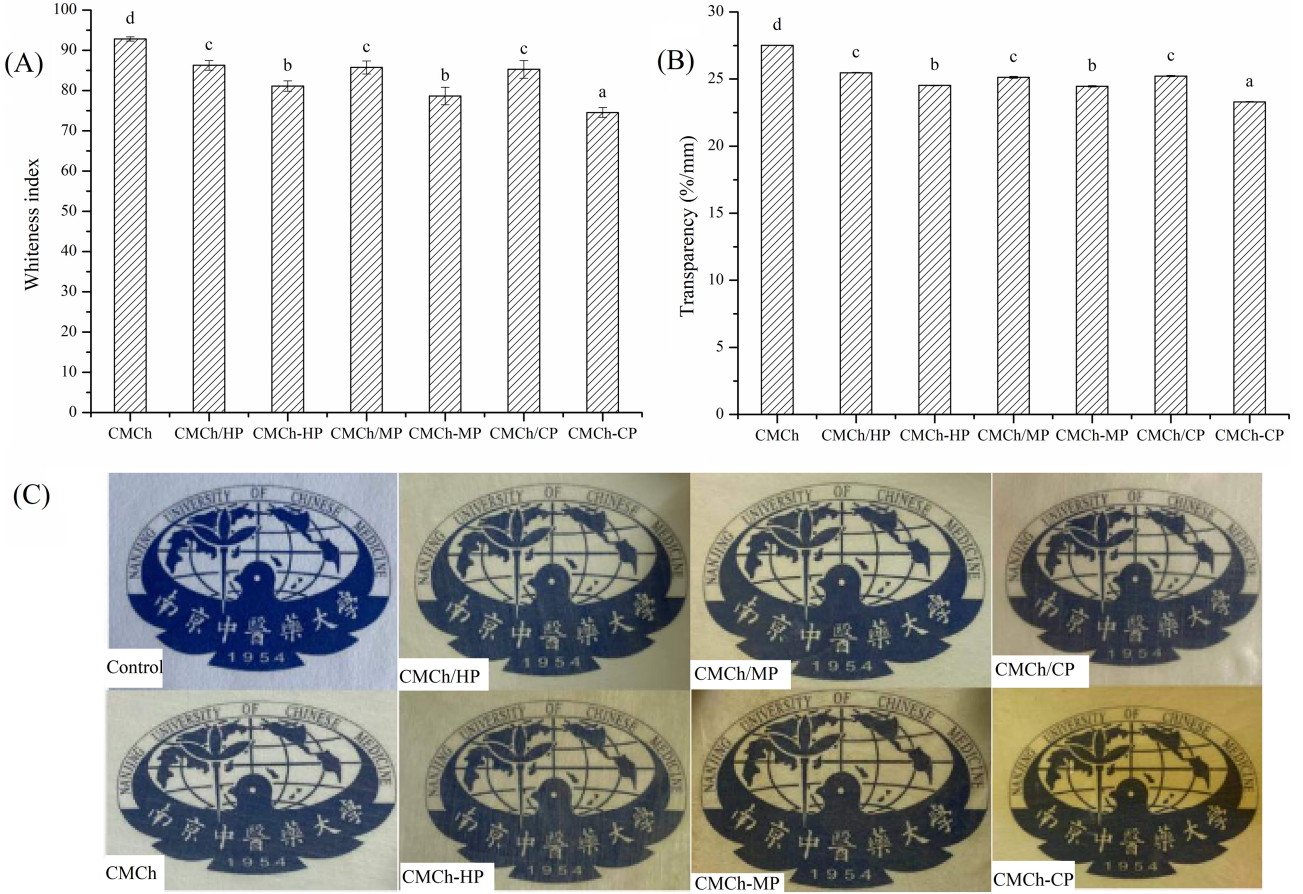
(A)
Whiteness index
100
90
80
70
60
50
40
30
20
10
0
d
c
b
c
b
c
a
CMCh
CMCh/HP
CMCh-HP
CMCh/MP
CMCh-MP
CMCh/CP
CMCh-CP
(B)
Transparency (%/mm)
30
25
20
15
10
5
0
d
c
b
c
b
c
a
CMCh
CMCh/HP
CMCh-HP
CMCh/MP
CMCh-MP
CMCh/CP
CMCh-CP
(C)
Control
CMCh/HP
CMCh/MP
CMCh/CP
CMCh
CMCh-HP
CMCh-MP
CMCh-CP

Figure 3

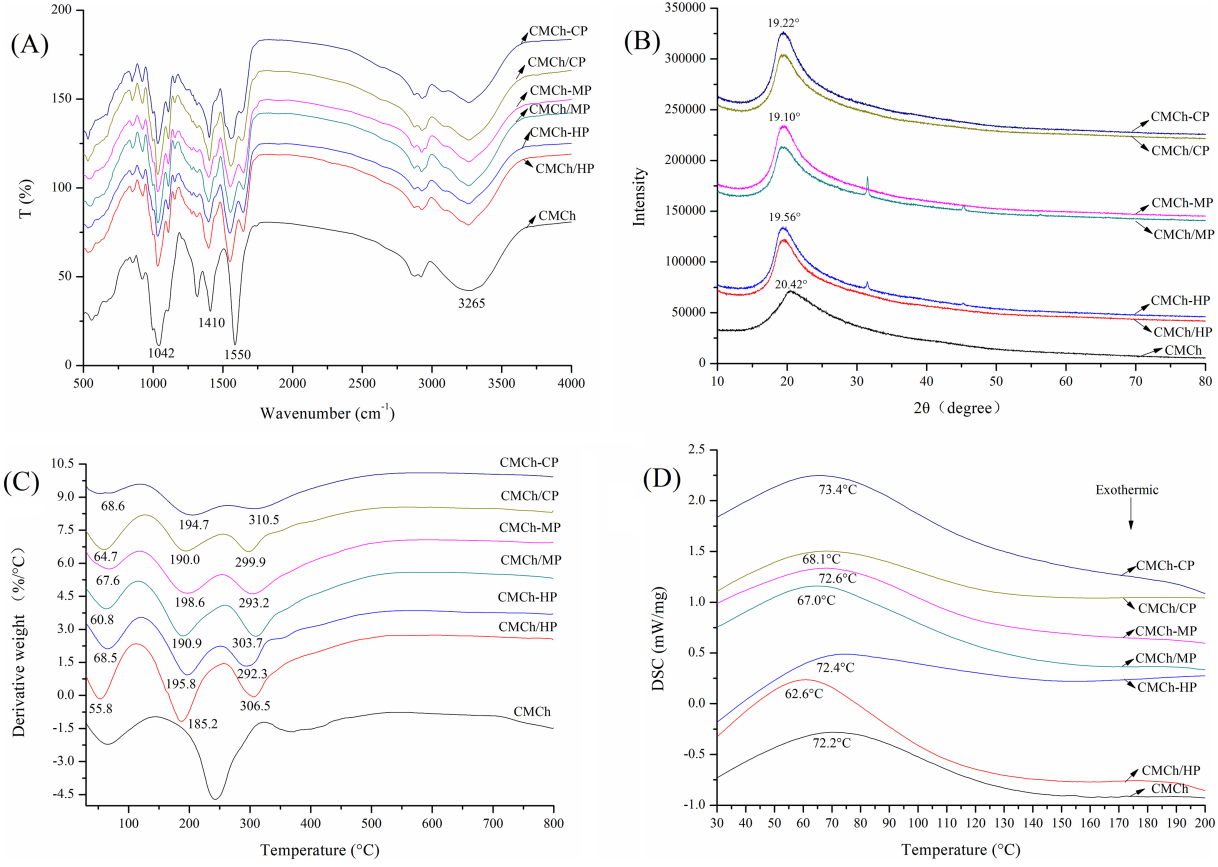
(A)
T (%)
Wavenumber (cm-1)
CMCh-CP
CMCh/CP
CMCh-MP
CMCh/MP
CMCh-HP
CMCh/HP
CMCh
1042
1410
1550
3265
(B)
Intensity
2θ（degree）
19.22°
19.10°
19.56°
20.42°
CMCh-CP
CMCh/CP
CMCh-MP
CMCh/MP
CMCh-HP
CMCh/HP
CMCh
(C)
Derivative weight （%/°C）
Temperature (°C)
68.6
194.7
310.5
64.7
190.0
299.9
67.6
198.6
293.2
60.8
190.9
303.7
68.5
195.8
292.3
55.8
185.2
306.5
(D)
DSC (mW/mg)
Temperature (°C)
Exothermic
73.4°C
68.1°C
72.6°C
67.0°C
72.4°C
62.6°C
72.2°C

Figure 4

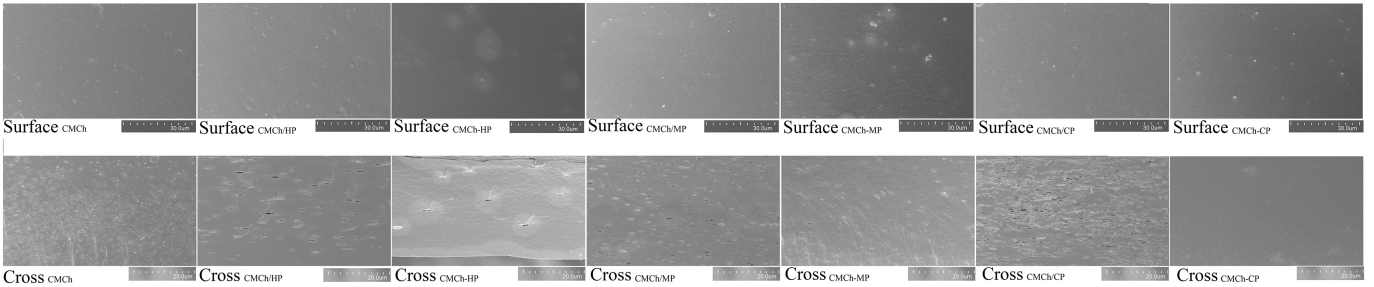
Surface CMCh
Surface CMCh/HP
Surface CMCh-HP
Surface CMCh/MP
Surface CMCh-MP
Surface CMCh/CP
Surface CMCh-CP
Cross CMCh
Cross CMCh/HP
Cross CMCh-HP
Cross CMCh/MP
Cross CMCh-MP
Cross CMCh/CP
Cross CMCh-CP

Figure 5

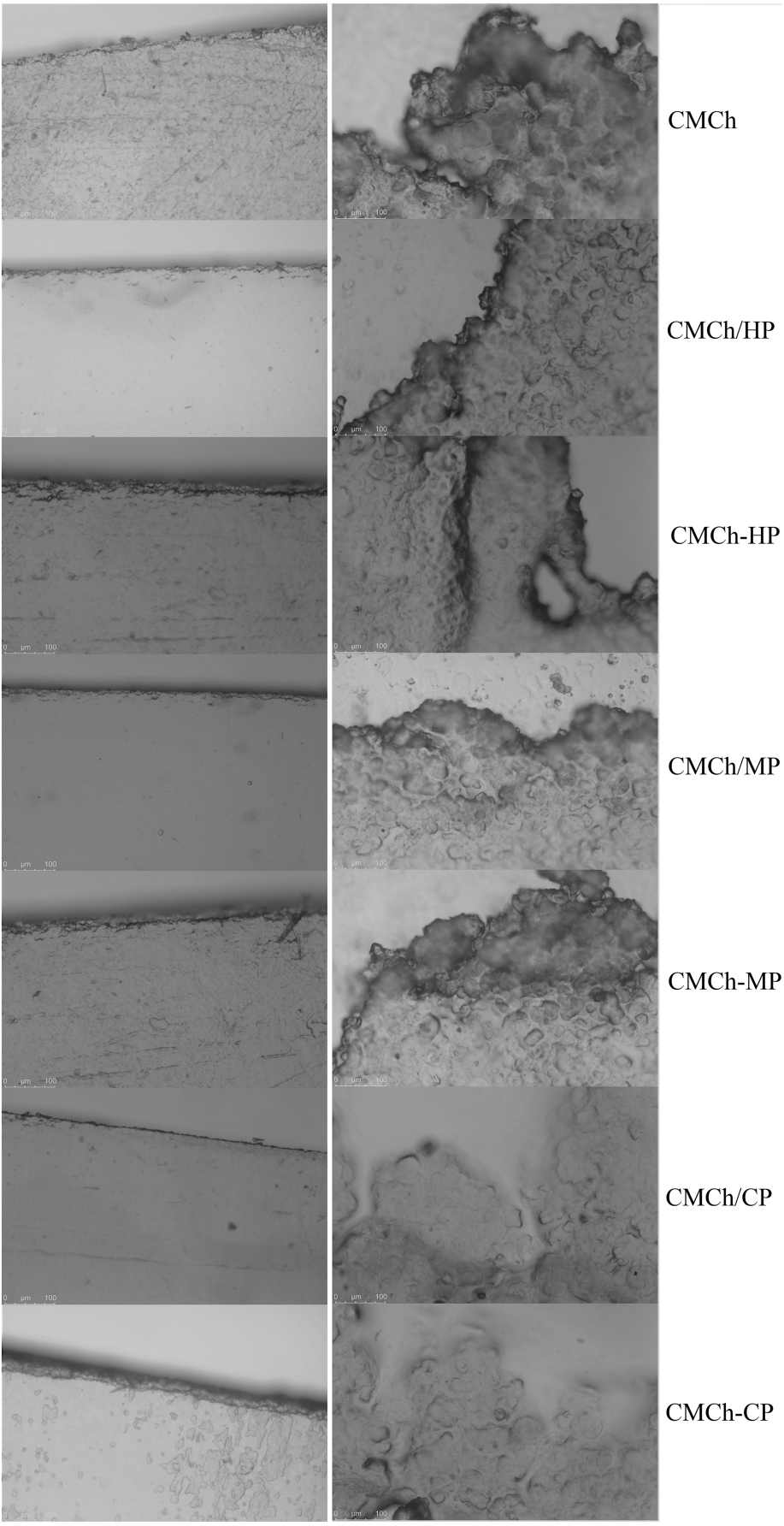
CMCh
CMCh/HP
CMCh-HP
CMCh/MP
CMCh-MP
CMCh/CP
CMCh-CP
0 days
30 days

Figure 6

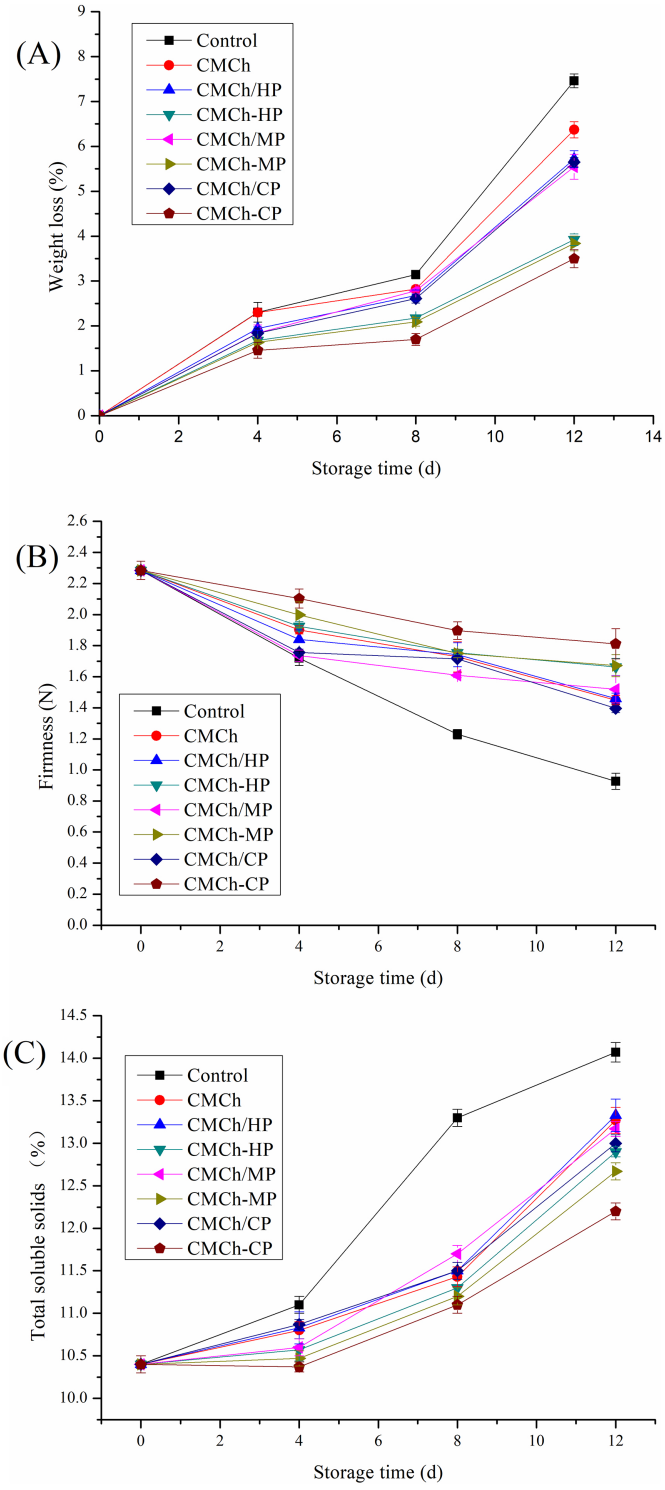
(A)
Control
CMCh
CMCh/HP
CMCh-HP
CMCh/MP
CMCh-MP
CMCh/CP
CMCh-CP
Weight loss (%)
Storage time (d)
(B)
Firmness (N)
Storage time (d)
(C)
Total soluble solids （%）
Storage time (d)

Figure 7